Compton scattering of 279.2-keV γ rays by K-shell electrons

G. Basavaraju, P. P. Kane, and Suju M. George

Physics Department, Indian Institute of Technology, Powai, Bombay 400 076, India

Coincidence techniques have been employed in a detailed study of Compton scattering of 279.2-keV γ rays by K-shell electrons of tin and gold. Double-differential cross sections at four angles have been determined from about 30 keV to the kinematic limit. In the case of gold, clear evidence has been obtained for the infrared divergence effect predicted by Gavrila, and for Compton defects towards lower energies. The data obtained with tin do not show significant infrared divergence or Compton defects. The widths of the fully developed quasi-Compton peaks are about 85 and 55 keV in the case of gold and tin, respectively. A detailed investigation has been made of possible false coincidences arising from secondary processes. Energy-integrated single-differential cross sections have also been determined. Comparisons with other experimental data and with results of theoretical calculations have been presented. The experimental cross sections in the regime of low outgoing photon energies are much larger than nonrelativistic and relativistic theoretical predictions. The experimental data above about 100 keV are in much better agreement with the relativistic second-order S-matrix calculations of Whittingham, although at some angles deviations of about 30% are noticeable. The desirability of additional relativistic calculations and measurements with extremely thin targets has been pointed out.

I. INTRODUCTION

Experimental and theoretical investigations of Compton scattering by bound atomic electrons[1-4] were initiated very soon after the discovery of the Compton effect. These early investigations were concerned with the effect of electron binding in atoms of low atomic number Z on the scattering of comparatively low-energy x rays, e.g., molybdenum $K\alpha$ x rays of 17.4 keV. During the past 25 years, thallium-activated sodium iodide detectors or high-resolution semiconductors detectors and coincidence techniques have been used to extend the scope of the early investigations to the study of Compton scattering of higher-energy γ rays by inner-shell electrons of high-Z atoms.

One technique of studying the scattering by inner-shell electrons has relied on the use of a high-resolution semiconductor detector to determine the whole atom Compton profile at momentum transfers or outgoing photon energies much larger than that corresponding to the strong Compton peak arising from all atomic electrons.[5-11] In these experiments, the Compton profile intensity has revealed noticeable sharp breaks at higher and higher values of energies on account of constraints imposed by the K- and L-shell binding energies. Since the intensity in the neighborhood of the breaks is smaller by several orders of magnitude than that at the peak, accurate determination of the intensity variation in the neighborhood of the breaks requires very strong sources, typical strengths being about 100 Ci, and targets of thickness greater than about 0.1 g/cm^2. Results at outgoing photon energies lower than about 100 keV have not been obtained. Further, the analysis of the data has been performed with the help of an impulse approximation or a form factor approximation. Neither of these approximations has been justified in a general way in the case of strongly bound inner-shell electrons.

Electronic coincidence techniques provide another and more direct method of studying this process in the case of individual atomic shells. For example, the scattered γ rays are detected in coincidence with the K x rays accompanying K-shell Compton scattering within an interval of the order of 10^{-17} sec in the case of high-Z atoms. In this way, K-shell scattering events are distinguished electronically from other scattering contributions. Therefore, it becomes possible to use smaller source strengths and thinner targets and thus to minimize the detection of undesirable secondary events. Coincidence techniques have been employed for an incident photon energy as low as 59.4 keV,[12,13] or as high as 1.12 MeV.[14,15] With 279.2-keV γ rays, coincidence studies have been reported for K-shell scattering from silver, samarium, tantalum and gold,[16,17] from erbium, tungsten, platinum, bismuth, and thorium,[18-21] and from tantalum and lead.[22,23] In the case of the above-mentioned experiments performed with 279.2-keV γ rays, pulse-height distributions of the emergent γ rays in the coincidence gated mode have been published in only a few cases and even in these rare cases do not extend downwards below about 100 keV. As a result, there is not much information concerning the width of the K-shell quasi-Compton peak and the Compton defect, and no information concerning the predicted infrared divergence (IRD) effect at low outgoing photon energies. Considerable information regarding these features was obtained[24] with 320-keV γ rays. However, contrary to expectations based on Fourier transforms of charge distributions of Doppler broadening arising from spreads in electron momenta, the width of the quasi-Compton peak was found to be larger in the case of holmium ($Z = 67$) than in the case of gold ($Z = 79$). In the limit of low outgoing photon energy, theory[25,26] predicted a proportionality of

the double-differential scattering cross section to the K-shell photoeffect cross section, that is, an IRD effect strongly increasing with Z. Yet the experimental results at 320-keV showed the largest IRD effect in the case of holmium. Further, the origin of a strong K x-ray peak in the emergent photon spectra was not studied.

In view of this situation, and the fact that L-shell Compton scattering data at 279.2 keV obtained with a gold target were available[27,28] we considered it worthwhile to undertake a detailed study of K-shell scattering at the same energy. Brief reports concerning a few aspects of this work have been presented earlier.[28-31] Here we report substantial new information in the angular range from 44° to 115°, mainly in the case of tin and gold targets, and analyses of data concerning both double-differential and single-differential Compton scattering cross sections.

The experimental details and results have been described in Sec. II. The underlying theoretical approaches are mentioned briefly in Sec. III. Results and conclusions are discussed in Sec. IV.

II. EXPERIMENTAL DETAILS

A. Experimental arrangement

^{203}Hg sources of about 700-mCi initial strength giving 279.2-keV γ rays were used in the present work. The source has a half-life of 47 days. Therefore, during the course of the experiment, several similarly prepared sources had to be employed. The precise value of the source strength does not have to be known when use is made of a normalization technique involving Compton scattering measurements in the single mode with a low-Z target such as aluminum. This well-known technique will be briefly mentioned in Sec. II B. The source is housed in a lead cylinder of 18 cm diameter and 18 cm height, the collimator having 0.8 cm diameter and 10 cm length. The collimated γ rays were incident on a target at a distance of about 20 cm from the source. The distance of the target from a thin γ-ray detector was usually 10 cm, whereas the target to γ-ray counter distance varied from 10.5 cm at 115° to 22 cm at 44°. Graded shielding of lead, brass, and aluminum was used throughout in order to suppress the detection of extraneous characteristic x rays. The arrangement for measurements at 115° is shown in Fig. 1.

The K x rays were detected with a NaI(Tl) crystal of 4.4 cm diameter and 0.3 cm thickness and equipped with 0.013-cm-thick beryllium window, hereafter designated as the x-ray detector. This detector can of course detect higher-energy γ rays but with considerably smaller efficiency. Further, a single-channel analyzer coupled to the output of this detector selected only pulses with heights corresponding to the photopeaks of K x rays of the target. In exploratory and much shorter measurements with a holmium target, the K x rays were detected with a high-resolution Si(Li) detector of lower efficiency (about 0.2). The purpose of these exploratory measurements will be described in Sec. II C.

The thicker detector, hereafter designated as the γ-ray counter, was a 4.4-cm-diameter by 5.1-cm-height NaI(Tl) crystal with 0.025-cm-thick aluminum window. The detection of recoil electrons from the target was suppressed by this window, as well as by an aluminum absorber of 0.015 cm thickness placed in front of the x-ray detector window.

A conventional fast-slow coincidence circuit was used
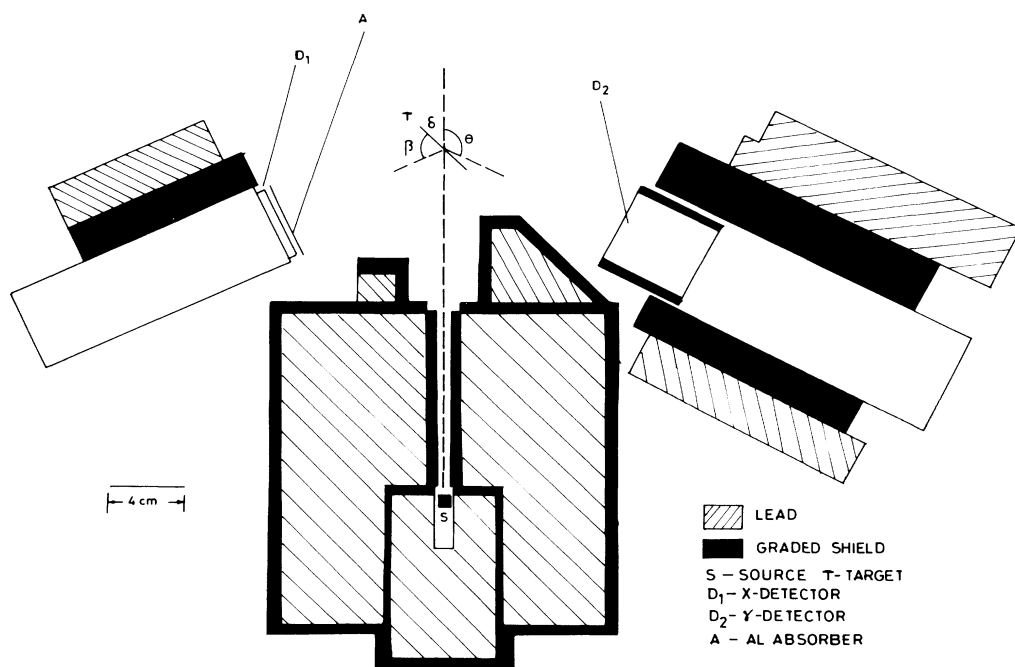
FIG. 1. Experimental arrangement at 115°.

TABLE I. Integrated coincidence count rates above 100 keV per hour. Data at 54° not shown. It should be noted that source strengths were different for different cases. Counting times for each measurement were about 50 h.

Angles (degrees)	Target	N^T	N_{ch}^T	N^{Al}	N_{ch}^{Al}	$N_t = N^T - N_{ch}^T - (N^{Al} - N_{ch}^{Al})$
44	gold	154.4±1.74	96.7±1.74	29.5±0.86	3.15±0.41	31.35±2.64
	tin	51.28±1.19	19.96±0.88	12.19±0.60	0.49±0.19	19.66±1.61
90	gold	31.75±0.74	13.25±0.49	4.93±0.49	0.53±0.17	14.10±1.03
	tin	47.55±0.96	31.04±0.81	1.10±0.28	0.51±0.29	15.92±1.32
115	gold	186.25±2.05	65.79±1.41	49.07±1.22	11.14±0.86	83.5±2.91
	tin	126.89±1.62	75.21±1.25	9.21±0.63	1.28±0.34	43.75±2.17

to record events detected by the γ-ray counter in coincidence with K x rays detected by the x-ray detector. After a careful study, the resolving time of the fast coincidence circuit was chosen to be 100 nsec in order to ensure 100% coincidence efficiency over pulse heights varying by a factor of 20 from about 15 to 300 keV. The resolving time of the slow coincidence circuit was 4 μsec. The output of the slow coincidence unit was used to gate a 512-channel pulse-height analyzer, the input to the analyzer being an amplified pulse from the γ-ray counter. The net coincidence counts N_t are obtained from Eq. (1):

$$N_t = N^T - N_{ch}^T - N_f , \qquad (1)$$

where N^T, N_{ch}^T, and N_f represent, respectively, the coincidence counts obtained with the target under study, the chance coincidence counts with the same target, and the false coincidence counts. Usually, the target Z-independent false coincidence counts are estimated as $(N^{Al} - N_{ch}^{Al})$, where N^{Al} and N_{ch}^{Al} indicate the coincidence counts obtained with an equivalent aluminum target and the corresponding chance coincidence counts. The designation "equivalent aluminum target" means an aluminum target having the same number of electrons as the target under study. Values of N^T, N_{ch}^T, N_f, and N_t for energies higher than 100 keV are indicated in Table I. In the lower-energy regime, the relative contribution of N_f is much smaller but there is a possible Z-dependent contribution of false counts. As mentioned in Sec. II C, this latter contribution was investigated in detail for the first time and was found to be less than about 6%. The possible origins of the target Z-independent false counts N_f have been discussed by several authors[32–34] in connection with earlier work performed with 661.6-keV γ rays and are therefore not discussed here again.

B. Pulse-height data and determination of cross sections

Pulse-height data obtained in the single mode with an aluminum target were used to determine the shape, the width, and the position of the Compton peak arising from weakly bound electrons. Data obtained at 115° are shown in Fig. 2. The measured width of about 25 keV represents the combined effect of finite angular acceptance and the resolution of the γ-ray counter system. Compton defects were measured with reference to the positions of the peaks observed with aluminum targets in the single mode and designated as k_F. Measurements made with

12.85 and 40.5-mg/cm² gold targets, and 20.2 and 40.5-mg/cm² aluminum targets showed that, within the experimental error of about 2%, counts corrected for target transmission in different pulse-height regions were proportional to the target thickness. Thus secondary effects are of negligible importance in the single-mode measurements.

Pulse-height data obtained at 115° in the coincidence gated mode with 40.5-mg/cm² gold target and 18.8-mg/cm² tin target are presented in Figs. 3 and 4, respectively. The peak representing quasi-Compton scattering from K-shell electrons is much broader than the peak observed in the single mode with an aluminum target. Further, as expected, the width of the gold peak is much larger than that of the tin peak. The position of the latter is the same as that of the free electron peak within the experimental error of about ±7 keV, whereas the gold peak is shifted toward lower energies. It should be noted that the intensity drops to zero near the energy $(k_0 - B_K)$, where the incident energy k_0 is 279.2 keV, and the K-shell binding energy B_K is 29.2 and 80.7 keV in the case of tin and gold, respectively. The observed cutoff behavior is consistent with energy conservation and the finite resolution of the γ-ray counter. At the smaller angles of
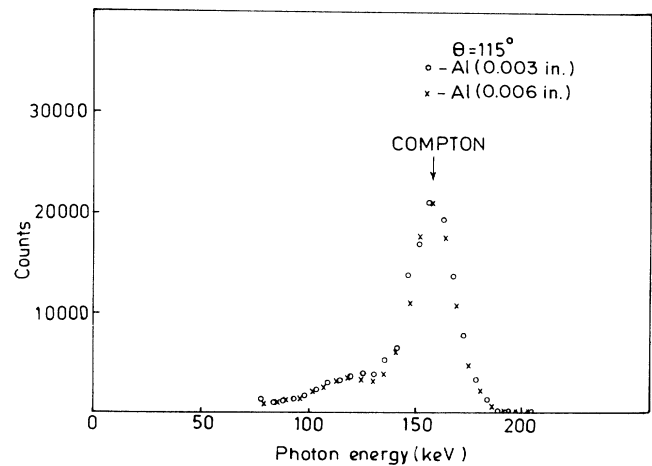
FIG. 2. Pulse-height data obtained at 115° in the singles mode with aluminum targets of different thickness. The two sets of data show that secondary contributions are negligible. The energy of the free electron Compton peak is indicated by the arrow labeled Compton.
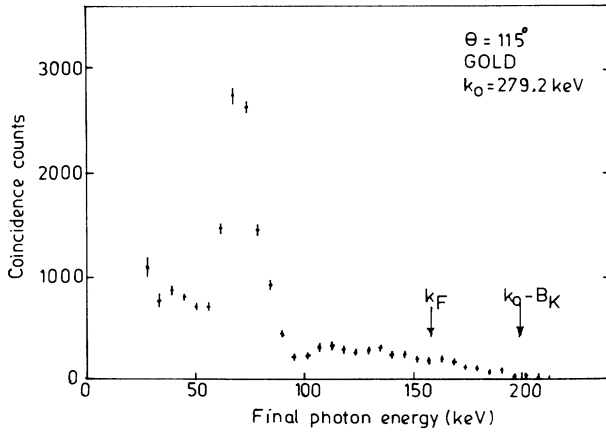
FIG. 3. Pulse-height data obtained at 115° in the coincidence gated mode with a gold target. k_F indicates the energy at which the free electron Compton peak is expected. The quasi-Compton peak arising from K-shell electrons is broadened, shifted toward an energy lower than k_F, and extends up to $(k_0 - B_K)$, where k_0 is the incident photon energy and B_K is the binding energy of gold K-shell electrons. Note also the K x-ray peak around 70 keV and counts increasing with decreasing energy below about 60 keV.

44° and 54°, the quasi-Compton peaks in the case of gold are eroded on the high-energy side by energy conservation requirements (see the discussion in Ref. 32).

Strong K x-ray peaks in the neighborhood of 70 keV in the case of gold and 26 keV in the case of tin are seen in Figs. 3 and 4, respectively. Below the K x-ray peak of gold, an increase of count rate with decreasing pulse height is clearly seen, in qualitative agreement with the predicted IRD effect. Since the low-energy-limit IRD cross section is expected to be proportional to the K-shell photoeffect cross section which varies approximately as
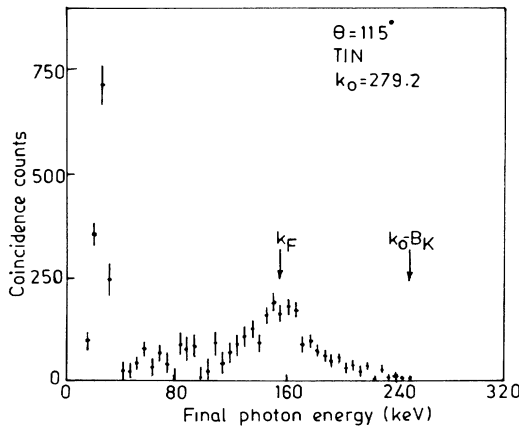
FIG. 4. Pulse-height data obtained at 115° in the coincidence gated mode with a tin target. Within experimental errors, the quasi-Compton peak position is the same as k_F. Note the K x-ray peak around 26 keV.

the fifth power of Z, we do not expect to observe a prominent IRD effect in the case of tin K-shell Compton scattering. This expectation is confirmed at all angles down to an energy as low as about 35 keV.

Pulse-height data of the type presented in Figs. 2,3, and 4 are used to obtain the double-differential scattering cross section $d^2\sigma_K/d\Omega\,dk$ for a K-shell electron,

$$\frac{d^2\sigma_K}{d\Omega\,dk} = \frac{\Delta N_t}{\Delta k}\frac{1}{N_S}\frac{n_{Al}}{n_K}\frac{\epsilon_\gamma^{Al}}{\epsilon_\gamma^K}\frac{a_\gamma^{Al}}{a_\gamma^K}\frac{1}{\eta_K}\frac{1}{\epsilon_K\Omega_K a_K \omega_K}\frac{d\sigma_{KN}}{d\Omega},$$

(2)

where ΔN_t is the number of net coincidence counts obtained with a given target in a small energy interval Δk of the order of 5 keV, N_S is the number of counts in the same period in the Compton peak determined in the single mode with a low-Z target such as that of aluminum, n_{Al} and n_K are, respectively, the numbers of electrons in the aluminum target and of K-shell electrons in the target under study, ϵ_γ^{Al} is the detection efficiency for photons Compton scattered by aluminum, ϵ_γ^K is the detection efficiency for K-shell scattered photons of energy in the middle of the chosen interval Δk, a_γ^{Al} and a_γ^K are the transmission factors corresponding to aluminum scattering and to the given target scattering, η_K is the single-channel analyzer acceptance factor for target K x rays, ω_K is the K-shell fluorescence yield of the target and is known to about 1.5% accuracy, ϵ_K, Ω_K, and a_K are, respectively, the detection efficiency, solid angle, and transmission factor for target K x-ray detection, and $d\sigma_{KN}/d\Omega$ is the Klein-Nishina prediction for scattering by free and stationary electrons. The error in N_S was usually less than 1.5%. The statistical error in ΔN_t was kept below about 15%, the total counting time at each angle being about 200 h. The statistical error below 100 keV was much less than the above-mentioned value. The error in the product $\eta_K\epsilon_K\Omega_K a_K$ is about 7% and is relevant for absolute values of cross sections. However, this error does not affect the relative values of $d^2\sigma_K/d\Omega\,dk$ or the angular variation of the single differential cross section. The general method of unfolding pulse-height distributions in order to obtain double-differential cross sections has been described in Ref. 15. However, as argued in Ref. 24, the above-mentioned method of obtaining double-differential cross sections is suitable for γ energies below about 300 keV. After integration of $d^2\sigma_K/d\Omega\,dk$ from a selected lower threshold energy to higher energies, the value of the single differential cross section $d\sigma_K/d\Omega$ is obtained. The statistical error in $d\sigma_K/d\Omega$ was less than 5% in some cases and less than about 8% in all cases.

C. Low-energy and K x-ray data in coincidence gated mode

We shall now discuss the intensities of K x rays and of lower-energy photons determined with the γ-ray counter in the coincidence gated mode. It is necessary to understand whether these events have a purely primary origin associated with K-shell Compton scattering or also a secondary contribution arising from target-Z-dependent false events produced by bremsstrahlung and/or K-shell

ionization caused by electrons released through photoeffect or Compton scattering. The approximate $1/k$ dependence of the IRD contribution is also expected in the case of the secondary bremsstrahlung. Following an approach suggested by earlier higher-energy work,[32,14] we performed coincidence measurements with 12.85 and 40.5 mg/cm^2 gold targets at 90°. The low-energy and the K x-ray counts, corrected for target transmission, were found to be proportional to the target thickness within an experimental error of less than 10%. However, unlike in the case of the higher-energy work, the approximate proportionality observed with 279.2-keV γ rays in the present experiment cannot by itself immediately lead to the suggestive conclusion that secondary contributions were negligible. The reason is that even the thinner target thickness (see Fig. 1 and the inclination of the target to beam directions) is comparable to the ranges of the photoelectrons and Compton electrons in the present case. Therefore, a detailed analysis is necessary before firm conclusions can be reached. This has in fact been done by us and reported in a separate publication[35] which lists a large number of possible sources of target-Z-dependent false counts, shows that only a few of these are likely to be of any significance, and then describes the estimates of bremsstrahlung and of secondary K x-ray intensities in the coincidence gated mode. Only the main conclusions of that analysis need to be stated here for the sake of completeness.

The measured energy distributions above about 100 keV were shown to be almost free of secondary contributions. Between 25 and 100 keV, the secondary contributions were estimated to be at most about 6%, in agreement with the observed approximate proportionality to target thickness. Thus K x rays detected by the γ-ray counter in the coincidence gated mode were shown by this analysis to be mainly associated with low-energy IRD photons accepted by the single-channel analyzer window at the output of the x-ray detector.

An independent experimental check of the last mentioned point was carried out in the following manner. Instead of the thin NaI x-ray detector, a high-resolution but lower-efficiency Si(Li) detector of 0.5 cm thickness was used for the detection of holmium K x rays. In this check, a holmium target was used instead of gold in order to ensure reasonable detection efficiency for the K x rays. Then the single-channel-analyzer window width could be chosen as small as 7 keV instead of a value of about 40 keV chosen in connection with the NaI detector. Therefore, the intensity of IRD photons accepted by the single-channel analyzer was substantially reduced. As expected, this resulted indeed in a correspondingly smaller intensity of K x rays recorded by the γ-ray counter in the coincidence mode.

D. Experimental results

The deduced energy distributions of emergent photons are displayed in Figs. 5, 6, and 7 for gold at 44°, 90°, and 115°, and in Fig. 8 and 9 for tin at 90° and 115°. Other data at 44° and 54° are not shown. Note that the low-
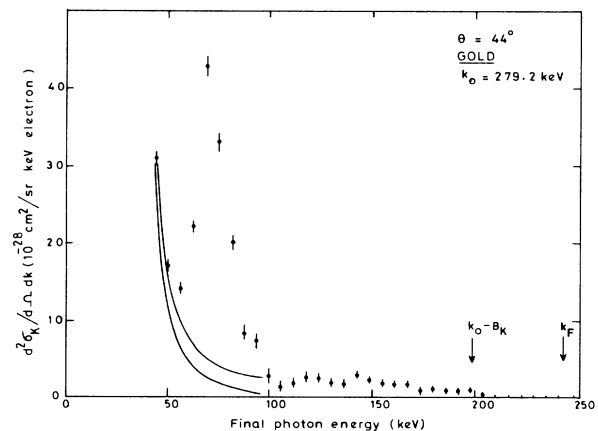
FIG. 5. Double-differential cross section for Compton scattering of 279.2-keV γ rays by K-shell electrons of gold at 44°. Below about 90 keV the cross section due to Compton scattering alone, corrected for secondary contributions, is expected to lie within the two solid curves (see Sec. II C).

energy data in the case of tin are not shown below about 40 keV, since in this case only the K x-ray feature has been clearly seen (see Fig. 4). Within the experimental error of ± 7 keV, the Compton defect is zero in the case of tin. The Compton defects towards low energies in the case of the gold target are about 55 and 30 keV at 90° and 115°, respectively. At 44° and 54°, the quasi-Compton peaks in the case of gold are eroded on the high-energy side on account of the K-shell binding-energy constraint. The full widths at half maximum (FWHM) of the fully developed quasi-Compton peaks are about 85 keV in the case of gold and about 55 keV in the case of tin. As pointed out in the Introduction, these observations are consistent with simple theoretical arguments. It should be noted that the FWHM reported in an earlier experiment with tungsten (Ref. 18) was surprisingly and inexplicably
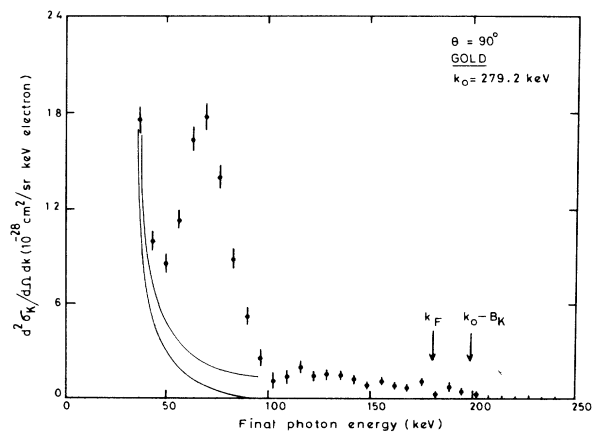
FIG. 6. Same as for Fig. 5, except that scattering angle is 90°.

TABLE II. Different experimental results for the ratio of the cross section for the Compton scattering of 279.2-keV γ rays by a K-shell electron to the theoretical Klein-Nishina prediction for electrons at rest. (For high-Z elements.)

Angle of scattering (degrees)	Present work gold[a]	gold[b]	Other data platinum[c]	bismuth[d]	lead[e]
20		0.20±0.021			
30			0.25±0.02	0.40±0.07	0.28±0.05
44	0.37±0.04				
50			0.45±0.10	0.41±0.035	0.52±0.05
55		0.317±0.029			
70			0.62±0.06	0.56±0.035	0.34±0.05
90	0.57±0.06	0.378±0.028			
105			0.78±0.08	0.75±0.04	
110					0.40±0.06
115	0.96±0.08				
125		0.426±0.030	0.88±0.06	0.92±0.04	
130					0.51±0.07
150			1.16±0.12	1.03±0.035	0.51±0.04
160		0.449±0.024			

[a]The quoted error is the total error. Threshold is 100 keV.
[b]Reference 16. The quoted error is statistical. Threshold is not stated.
[c]Reference 21. The quoted error is statistical. Values read from graph. Threshold is not stated.
[d]Reference 19. The quoted error is statistical. Values read from graph. Threshold is not stated.
[e]Reference 23. The quoted error is the total error. Values read from graph. Threshold is 100 keV.

smaller than the width measured in the single mode with an aluminum target. As already pointed out in Sec. II B clear evidence for IRD is obtained only in the case of the gold target.

From data of the type presented in Figs. 5–9, single differential cross sections for K-shell electron scattering can be obtained for any selected threshold energy. At 115°, when the threshold is lowered from 110 to 100 keV, the single-differential cross section increases by about 10% in the case of gold and 3% in the case of tin. For reporting the results, we have used 100 keV as the threshold in the case of both tin and gold. The ratio of the K-shell electron scattering cross section to the Klein-Nashina prediction for free and stationary electrons is designated as the cross-section ratio and indicates the gross effect of binding on the cross section. In Tables II and III, we present the values of the cross-section ratio determined in this experiment along with the values re-
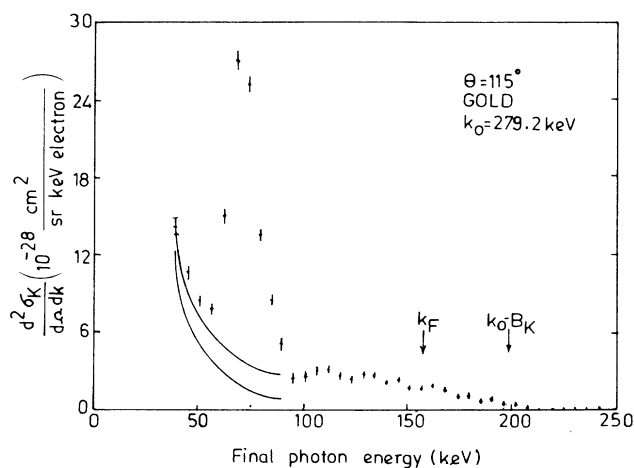
FIG. 7. Same as for Fig. 5, except that the scattering angle is 115°.
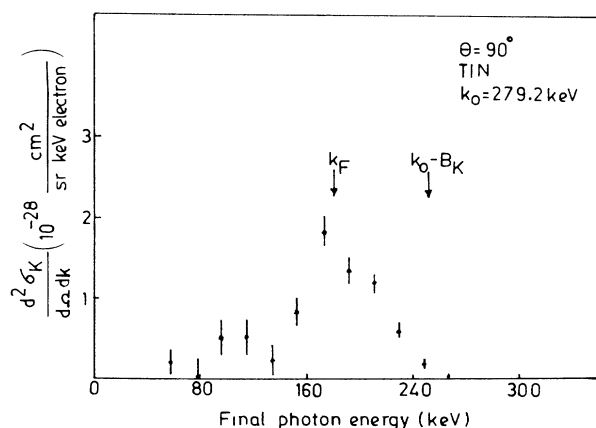
FIG. 8. Double-differential cross section or Compton scattering of 279.2-keV γ rays by K-shell electrons of tin at 90°. The data in the neighborhood of and slightly above the K x-ray peak are not shown.
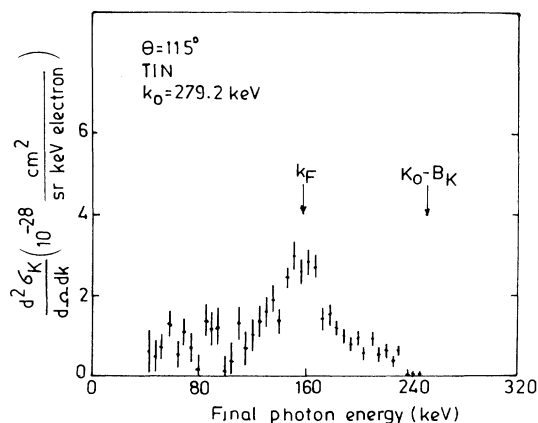
FIG. 9. Same as for Fig. 8, except that the angle of scattering is 115°.

ported by other authors for elements with similar Z values. Since coincidence efficiencies and low-energy thresholds have not always been mentioned by other authors, precise comparisons are rather difficult. Following observations can however be made. The values of Pingot for high-Z elements and of Singh et al. for lead are generally lower and strikingly so at large angles. As far as variation of the cross-section ratio with angle is concerned, the trends are similar in all data. Further, it can be stated that, except for bismuth at 150°, all cross section ratios measured with 279.2-keV γ rays are equal to or less than unity and that they increase with increasing angle of scattering in most cases.

III. THEORETICAL CALCULATIONS

Within the framework of nonrelativistic theory, the interaction of an electron with electromagnetic radiation is represented by two terms, namely, $e^2A^2/2mc^2$ and $(-e/mc)\mathbf{p}\cdot\mathbf{A}$. These are designated as A^2 and $\mathbf{p}\cdot\mathbf{A}$ terms, respectively. The symbols e and m represent the charge and mass of an electron, $\mathbf{p}$ is the momentum operator, and $\mathbf{A}$ is the vector potential of the electromag-

netic radiation. The A^2 term, evaluated in first-order perturbation theory, leads to a generalized form-factor expression involving an initial bound electron state and a final continuum state. It is responsible for the quasi-Compton peak and does not give rise to any IRD effect. An evaluation of the $\mathbf{p}\cdot\mathbf{A}$ contribution in second-order perturbation theory has been carried out analytically for a hydrogenic atom.[25] The explicit numerical results obtained in the dipole approximation clearly revealed a significant IRD effect.

The nonrelativistic form-factor expression for the double-differential cross section was obtained by Schnaidt[36] for a point Coulomb potential:

$$\frac{d^2\sigma_K}{d\Omega\, dk} = \frac{r^2}{2}(1+\cos^2\theta)\frac{256a^6}{3}\frac{k}{k_0}$$

$$\times \frac{q^2(a^2+p^2+3q^2)}{[a^2+(p+q)^2]^3[a^2+(p-q)^2]^3}$$

$$\times \frac{\exp\left[-2\frac{a}{p}\tan^{-1}\left|\frac{2ap}{a^2+q^2-p^2}\right|\right]}{1-\exp(-2\pi a/p)}, \qquad (3)$$

where r is the classical radius of an electron, the energies are in mc^2 units, the momenta are in the mc units, q is the momentum transfer in scattering, p is the momentum of the electron ejected from the K shell, $a=Z\alpha$, $\alpha=e^2/\hbar c=1/137.039$, k and k_0 are the energies of the scattered and the incident photons, the binding energy B is $a^2/2$,

$$q=[k_0^2+k^2-2kk_0\cos\theta]^{1/2},$$

and

$$p=[2(k_0-k-B)]^{1/2}.$$

In a relativistic theory, the electron-photon interaction term is $(-e\boldsymbol{\alpha}\cdot\mathbf{A})$, where the operators $\boldsymbol{\alpha}$ represent the three well-known 4×4 Dirac matrices. An accurate evaluation of the contribution of this term in second-order perturbation theory has been carried out through partial-wave expansions of the photon and the electron states and an application of Green's function techniques originally developed by Brown and Mayers[37] for the treatment of elastic photon scattering. Such elaborate relativistic calculations have so far been done only for 279.2- and 661.6-keV γ rays in the case of samarium, tantalum, lead, and uranium targets.[38,39] On account of the complexity of the calculational procedure, these predictions cannot be scaled in a straightforward way to other energies, angles, and atomic number. In the recent calculation of Whittingham for 279.2-keV γ rays, the IRD effect is noticeable in the case of lead below about 60 keV. The magnitude of the IRD cross section is somewhat smaller than the predicted by Gavrila. However, as pointed out by Whittingham, the convergence of the radial integrals was poor, particularly for lower outgoing photon energies, i.e., higher electron energies. Whittingham predicts a Compton defect towards positive energies, the magnitude of the predicted defect being about 10% of the energy at the Compton peak.

TABLE III. Cross-section ratio for medium-Z elements.

Angle of scattering (degrees)	Present work tin[a]	Other data silver[b]
20		0.158±0.032
44	0.43±0.05	
54–55	0.61±0.07	0.542±0.043
90	0.70±0.08	0.844±0.075
115	0.89±0.08	
125		1.039±0.061
160		1.076±0.069

[a]The quoted error is the total error. Threshold is 100 keV.
[b]Reference 17. The quoted error is statistical. Threshold is not stated.

For illustrative purposes, we show in Fig. 10 some of the calculated energy distributions. The curve marked WH represents the results of Whittingham for 120° scattering by lead K-shell electrons. The remaining three distributions are calculated for gold K-shell electrons so that a comparison with the data presented in Fig. 7 can be easily made. The curves marked G and FF, respectively, represent Gavrila's nonrelativistic dipole approximation results and form-factor results calculated according to Eq. (3). As pointed out by Schumacher[5] and Whittingham[39], the relativistic form-factor predictions in the present case are larger than the nonrelativistic form-factor predictions by a factor of about 2 and are not shown in the figure.

In the dipole approximation, the matrix element of the A^2 term reduces to an overlap integral between the orthogonal initial and final electron states. Hence there is no quasi-Compton peak in the dipole approximation. It has been argued[25,40] that the p·A and the A^2 contributions should interfere constructively. An approximate estimate of the correct nonrelativistic prediction, labeled GFF, has been obtained by the addition of Gavrila's dipole approximation amplitudes for the p·A contribution and the nonrelativistic form-factor results. The nonrelativistic energy distribution labeled GFF is broader than the relativistic calculation of Whittingham. The GFF cross sections are substantially larger than the form-factor results marked FF. This result does not appear to have been pointed out earlier. It should also be noted that screening effects have not been completely taken into account in any of these treatments. An impulse approximation has often been used for larger momentum transfers. As pointed out in an earlier work,[41] the validity of this approximation for treating Compton scattering from K shells of large-Z atoms is rather limited in scope.

On the basis of the A^2 approximation and additional subsidiary assumptions, the single-differential scattering cross section for a K-shell electron is given in the form of Eq. (4):

$$\frac{d\sigma_K}{d\Omega} = S_K(q,Z)\frac{d\sigma_{KN}}{d\Omega} , \qquad (4)$$

where S_K indicates the incoherent scattering function for a K-shell electron and measures the reduction of the scattering probability on account of electron binding. Values of S_K have been given, for example, in Refs. 32 and 34. This approximation is expected to be of greater validity for incident photon energies smaller than mc^2 but much larger than the binding energy and for momentum transfers much smaller than mc. The validity of various approximations has to be really examined from the point of view of deviations from available predictions from accurate relativistic calculations.

IV. DISCUSSION OF RESULTS

Since the relativistic second-order S-matrix calculations are not available for gold and tin, the experimental data for double-differential cross sections presented in Figs. 5–9 cannot be directly compared with such calculations. However, in order to understand the trends, data in Fig. 7 for gold at 115° may, for example, be compared with cal-

culations presented in Fig. 10 for lead and gold at 120°. The origin of the prominent K x-ray intensity in the experimental data has been explained in Sec. II C. The curves in Fig. 10 are based on calculations of only the scattering cross sections and therefore do not include the associated K x-ray intensities. Our data show the same qualitative features as the calculations and the data of Spitale and Bloom for incident γ rays of 320 keV, namely, an IRD contribution, a broad quasi-Compton peak, and a cutoff due to energy conservation requirements.

The K x-ray intensity is relatively larger than that in the work of Spitale and Bloom, presumably on account of the smaller incident photon energy and the larger single-channel analyzer window width at the output of the x-ray detector (see Sec. II C). Experimental results regarding full widths at half maximum of quasi-Compton peaks and Compton defects are summarized in Sec. II D. The widths of about 85 keV measured in the case of gold are similar to those predicted by Whittingham but smaller than those obtained on the basis of form-factor theories.

In agreement with the predictions of Gavrila, the measured cross sections in the IRD regime are much larger for larger Z. In fact, the tin data have not shown a clearly discernible rise with decreasing emergent photon energy. The corresponding lower-energy cross sections deduced by Spitale and Bloom with a holmium target and with 320-keV γ rays are consistent with our results, if the photoeffect cross sections are scaled for different incident γ energies and target atomic numbers. The cross sections determined for gold by Spital and Bloom in the IRD regime are surprisingly smaller than their own values for holmium. The cross sections determined by us for gold and by Spitale and Bloom for holmium are about an order of magnitude larger than the nonrelativistic theoretical predictions such as those of Gavrila. In this connection,
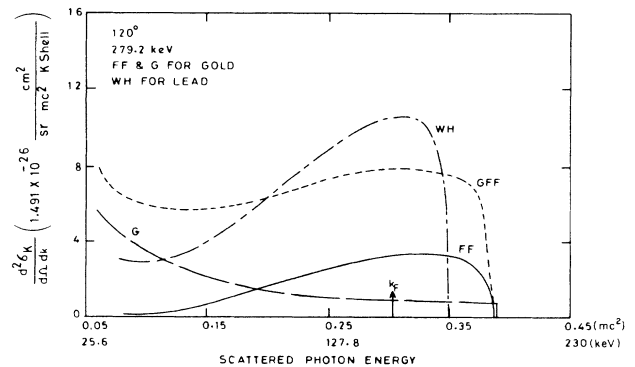
FIG. 10. Calculated double-differential cross sections for the Compton scattering of 279.2-keV γ rays through 120° by K-shell electrons. The vertical scale is the same as that chosen by Whittingham (Ref. 39). The curve labeled WH represents Whittingham's relativistic calculation for lead. The curve labeled G represents Gavrila's nonrelativistic calculation for gold in the dipole approximation. The curve labeled FF for gold is based on the nonrelativistic form-factor approximation. The curve labeled GFF represents the final nonrelativistic estimates for gold (see Sec. III).

it is necessary to add one remark. The low-energy-limit formula mentioned, but not derived, by Spitale and Bloom [Eq. (4) in their paper] predicts cross sections that are typically about six times as large as the values based on Gavrila's calculations. A low-energy-limit formula has been derived by Gavrila and kindly communicated to us privately. Note that this limit formula is in agreement with Eqs. (45) and (46) in a recently published review article.[42] This formula gives results in agreement with Gavrila's tabulated results. Thus, Eq. (4) in the paper of Spitale and Bloom appears to be incorrect. Therefore, as remarked above, the values of cross sections determined by Spitale and Bloom are also very much larger than theoretical predictions, although they have stated that their experimental values are in approximate agreement with theory. Our values for double-differential cross sections in the low-energy regime show much larger anisotropy than that predicted in the dipole approximation of Gavrila. It is certainly possible to argue in principle that the experimental values in the IRD regime are substantially incorrect. However, as shown in Ref. 35, this is unlikely. We feel that deviations between theory and experiments with 279.2- and 320-keV γ rays need to be studied further. Parenthetically, it may be mentioned that a deviation in the same direction but by a factor of only 2 was noticed in another experiment[40] concerned with whole atom scattering of about 8-keV x rays.

With a lower energy cutoff at 100 keV, we have evaluated the single-differential cross sections and therefrom the ratios of measured cross sections to the Klein-Nishina predictions for free electrons at rest. These ratios are listed in Tables II and III, along with data of other workers, for targets of similar *Z* values. Our values reveal fair agreement with the trends reported by Murty and coworkers.[18−21] Results from Refs. 16, 17, and 23 for tantalum, gold, and lead are systematically low, particularly

at large scattering angles. As mentioned in Sec. II D, the origin of this discrepancy is not clear. The experimental values of cross-section ratios generally increase with increasing angle of scattering. As a result, the *K*-shell electron Compton scattering cross section depends very weakly on scattering angle. This trend is broadly in agreement with the results of theoretical calculations. From Fig. 10, it is evident that the single-differential cross section obtained by integration of the double-differential cross section above 100 keV is not very different in the case of nonrelativistic and relativistic calculations labeled GFF (for gold) and WH (for lead), respectively. Thus, as is to be expected, the single-differential cross sections do not provide stringent comparisons with experimental results. The calculations of Whittingham on interpolation give values of 0.28, 0.68, and 0.70 for the cross-section ratios in the case of lead at 44°, 90°, and 115°, respectively. A definite deviation is thus discernible at 115° between experiment and theory. Relativistic second-order *S*-matrix calculations are not available for *Z* less than 62. Hence the cross-section ratios for tin are not compared with theory. It should be noted that the cross-section ratios for tin are in fair agreement with those of Pingot[17] for silver. Since the photon energy is about 0.6 times the rest energy of the electron, nonrelativistic calculations cannot really be considered reliable.

The present results show the need for further experimental work, particularly with very thin targets, as well as for more extensive relativistic calculations.

ACKNOWLEDGMENT

---

[1]F. L. Nutting, Phys. Rev. **36**, 1267 (1930).

[2]J. W. M. Dumond, Rev. Mod. Phys. **5**, 1 (1933).

[3]P. A. Ross and P. Kirkpatrick, Phys. Rev. **46**, 668 (1934).

[4]A. Sommerfeld, Phys. Rev. **50**, 38 (1936).

[5]M. Schumacher, Z. Phys. **242**, 444 (1971).

[6]T. Fukamachi and S. Hosoya, Phys. Lett. **41A**, 416 (1972).

[7]P. Rullhusen and M. Schumacher, J. Phys. B **9**, 2435 (1976).

[8]P. Pattison and J. R. Schneider, J. Phys. B **12**, 4013 (1979).

[9]P. Pattison and J. R. Schneider, Nucl. Instrum. Methods **158**, 145 (1979).

[10]A. Reineking, R. Wenskus, A. Baumann, D. Schaupp, P. Rullhusen, F. Smend, and M. Schumacher, Phys. Lett. **95A**, 29 (1983).

[11]M. J. Cooper, Rep. Prog. Phys. **48**, 415 (1985), and references mentioned therein.

[12]T. Fukamachi and S. Hosoya, Phys. Lett. **38A**, 341 (1972).

[13]M. Pradoux, H. Meunier, M. Avan, and G. Roche, Phys. Rev. A **16**, 2022 (1977).

[14]P. P. Kane and P. N. Baba Prasad, Phys. Rev. A **15**, 1976 (1977).

[15]P. N. Baba Prasad, P. P. Kane, and G. Basavaraju, Phys. Rev. A **15**, 1984 (1977).

[16]O. Pingot, Nucl. Phys. A **133**, 334 (1969).

[17]O. Pingot, J. Phys. (Paris) **33**, 189 (1972).

[18]D. S. R. Murty, V. Govinda Reddy, and E. Narasimhacharyulu, J. Phys. A **6**, 265 (1973).

[19]C. Nageswara Rao, V. Govinda Reddy, and D. S. R. Murty, J. Phys. B **10**, 47 (1977).

[20]D. S. R. Murty and V. Govinda Reddy, Physica **92C**, 137 (1977).

[21]S. T. P. V. J. Swamy and D. S. R. Murty, Physica **93C**, 145 (1977).

[22]B. Singh, P. Singh, G. Singh, and B. S. Ghumman, Ind. J. Phys. **58A**, 397 (1984).

[23]B. Singh, V. B. Acharya, and B. S. Ghumman, Pramana **24**, 743 (1985).

[24]G. C. Spitale and S. D. Bloom, Phys. Rev. A **16**, 221 (1977).

[25]M. Gavrila, Phys. Rev. A **6**, 1348 (1972); **6**, 1360 (1972).

[26]D. J. Botto and M. Gavrila, Phys. Rev. A **26**, 237 (1982).

[27]G. Basavaraju, S. M. George, and P. P. Kane, Nucl. Instrum. Methods **193**, 631 (1982).

[28]P. P. Kane, G. Basavaraju, and R. Venkatram, X-84 International Conference on X Ray and Inner Shell Processes in Atoms, Molecules and Solids, Leipzig, Part I, p. 130, 1984

(unpublished).

[29]P. P. Kane, G. Basavaraju, and S. M. George, X-82 International Conference on X Ray and Atomic Inner Shell Physics, Eugene, Oregon, p. 19, 1982 (unpublished).

[30]G. Basavaraju, P. P. Kane, S. M. George, and R. Venkatram, Ninth International Conference on Atomic Physics, Seattle, Washington, B-21, 1984 (unpublished).

[31]P. P. Kane, Fifth National Workshop on Atomic and Molecular Physics, Bombay, 1984 (unpublished).

[32]Z. Sujkowski and B. Nagel, Arkiv Fys. 20, 323 (1961).

[33]J. W. Motz and G. Missoni, Phys. Rev. 124, 1458 (1961).

[34]S. Shimizu, Y. Nakayama, and T. Mukoyama, Phys. Rev. 140A, 806 (1965).

[35]G. Basavaraju, P. P. Kane, and S. M. George, Nucl. Instrum. Methods A 255, 86 (1987).

[36]F. Schnaidt, Ann. Phys. (Leipzig) 21, 89 (1934).

[37]G. E. Brown and D. F. Mayers, Proc. R. Soc. London, Ser. A 234, 387 (1956).

[38]I. B. Whittingham, J. Phys. A 4, 21 (1971).

[39]I. B. Whittingham, Aust. J. Phys. 34, 163 (1981).

[40]Y. B. Bannett, D. L. Rapaport, and I. Freund, Phys. Rev. A 16, 2011 (1977).

[41]P. N. Baba Prasad and P. P. Kane, J. Nat. Bur. Stand. Sect. A 78, 461 (1974).

[42]T. Åberg and J. Tulkki, in Atomic Inner Shell Physics, edited by B. Crasemann (Plenum, New York, 1985), Chap. 10.